

# UC Irvine

## UC Irvine Previously Published Works

### Title

Long-Term Plasticity of Endocannabinoid Signaling Induced by Developmental Febrile Seizures

### Permalink

<https://escholarship.org/uc/item/9v14486v>

### Journal

Neuron, 39(4)

### ISSN

0896-6273

### Authors

Chen, Kang  
Ratzliff, Anna  
Hilgenberg, Lutz  
et al.

### Publication Date

2003-08-01

### DOI

10.1016/s0896-6273(03)00499-9

### Copyright Information

This work is made available under the terms of a Creative Commons Attribution License, available at <https://creativecommons.org/licenses/by/4.0/>

Peer reviewed

# Long-Term Plasticity of Endocannabinoid Signaling Induced by Developmental Febrile Seizures

Kang Chen,<sup>1</sup> Anna Ratzliff,<sup>1</sup> Lutz Hilgenberg,<sup>1</sup> Attila Gulyás,<sup>1,4</sup> Tamás F. Freund,<sup>4</sup> Martin Smith,<sup>1</sup> Thien P. Dinh,<sup>2</sup> Daniele Piomelli,<sup>2</sup> Ken Mackie,<sup>3</sup> and Ivan Soltesz<sup>1,\*</sup>

<sup>1</sup>Department of Anatomy and Neurobiology

<sup>2</sup>Department of Pharmacology  
University of California, Irvine  
Irvine, California 92697

<sup>3</sup>Department of Anesthesiology  
University of Washington  
Seattle, Washington 98195

<sup>4</sup>Institute of Experimental Medicine  
Hungarian Academy of Sciences  
Budapest  
Hungary

## Summary

Febrile (fever-induced) seizures are the most common form of childhood seizures, affecting 3%–5% of infants and young children. Here we show that the activity-dependent, retrograde inhibition of GABA release by endogenous cannabinoids is persistently enhanced in the rat hippocampus following a single episode of experimental prolonged febrile seizures during early postnatal development. The potentiation of endocannabinoid signaling results from an increase in the number of presynaptic cannabinoid type 1 receptors associated with cholecystokinin-containing perisomatic inhibitory inputs, without an effect on the endocannabinoid-mediated inhibition of glutamate release. These results demonstrate a selective, long-term increase in the gain of endocannabinoid-mediated retrograde signaling at GABAergic synapses in a model of a human neurological disease.

## Introduction

A central question in understanding the neurobiological consequences of seizures that take place during brain development concerns the precise nature of the long-term alterations in GABAergic synaptic transmission. Systematic prospective studies carried out in a novel experimental model system of prolonged (lasting more than 15 min) febrile seizures in the developing rat brain revealed a persistent, presynaptic, protein kinase-A-dependent increase in the perisomatic GABAergic transmission in CA1 pyramidal cells (Chen et al., 1999). Furthermore, experimental febrile seizures also resulted in a long-term increase in the hyperpolarization-activated, depolarizing conductance  $I_h$  in the postsynaptic membrane that limited the efficacy of the potentiated perisomatic GABAergic inputs in a frequency-dependent manner (Chen et al., 2001). In addition to distinct pre- and postsynaptic mechanisms of plasticity, seizures in development may also persistently alter retrograde signal-

ing at GABAergic synapses. Endocannabinoid-mediated retrograde signaling, in particular, has been shown to potently regulate transmitter release (Hájos et al., 2000; Hoffman and Lupica, 2000; Wilson and Nicoll, 2001; Wilson et al., 2001; Kreitzer and Regehr, 2001; Ohno-Shosaku et al., 2001). The signaling mechanism involves the calcium-dependent, postsynaptic synthesis and the subsequent rapid release of endocannabinoids, such as the fatty ethanolamide, anandamide (Di Marzo et al., 1994), or the monoglyceride 2-arachidonoylglycerol (2-AG) (Stella et al., 1997), which cross the synaptic cleft and bind to cannabinoid type 1 (CB-1) receptors on the presynaptic terminal to decrease transmitter release through a G protein-mediated pathway. This signaling cascade is triggered by a transient depolarization of the postsynaptic neuron and results in the endocannabinoid-mediated transient depression of neurotransmitter release, a process termed depolarization-induced suppression of inhibition (DSI, in the case of GABAergic synapses) (Pitler and Alger, 1992) or depolarization-induced suppression of excitation (DSE, for glutamatergic synapses) (Ohno-Shosaku et al., 2002).

Here we show that a single episode of hyperthermia-induced prolonged seizures at postnatal day 10 (P10) leads to a novel form of long-term plasticity involving the enhancement of endocannabinoid-mediated suppression of GABA (but not glutamate) release, due to a persistent upregulation of CB1 receptors selectively on cholecystokinin (CCK)-containing, perisomatic inhibitory terminals synapsing on principal cells in the hippocampus. To our knowledge, these findings constitute the first evidence that the endocannabinoid system can be persistently modified in cortical networks.

## Results

### Long-Term Enhancement of Depolarization-Induced Suppression of Inhibition

Depolarization of CA1 pyramidal cells from control animals for 500 ms resulted in a transient depression of the spontaneous, GABA<sub>A</sub> receptor-mediated, inhibitory postsynaptic currents (sIPSCs), a phenomenon known as DSI (Pitler and Alger, 1992) (Figure 1A, control; recordings were in the presence of the glutamate receptor antagonists 10  $\mu$ M APV and 5  $\mu$ M CNQX and 5  $\mu$ M of the cholinergic muscarinic agonist carbachol to boost sIPSC frequency). Compared to controls, DSI was significantly increased both in magnitude and duration in age-matched littermates that had hyperthermia-induced experimental febrile seizures (HT) 1 week before the recording session (Figures 1A and 1B; DSI amplitude in control: 20.2%  $\pm$  2.7%, expressed as percent decrease in sIPSC charge transfer following the depolarizing pulse, with respect to the prepulse control period; DSI in HT: 33%  $\pm$  3.7%; decay time constant of DSI in control: 2.2 s; in HT: 12.5 s; control:  $n$  = 11 cells from three animals; HT:  $n$  = 10 cells from four animals). To our knowledge, this is the first demonstration that DSI can be altered in a persistent manner (i.e., lasting at least 1 week; for longer time points, see below).

\*Correspondence: isoltesz@uci.edu

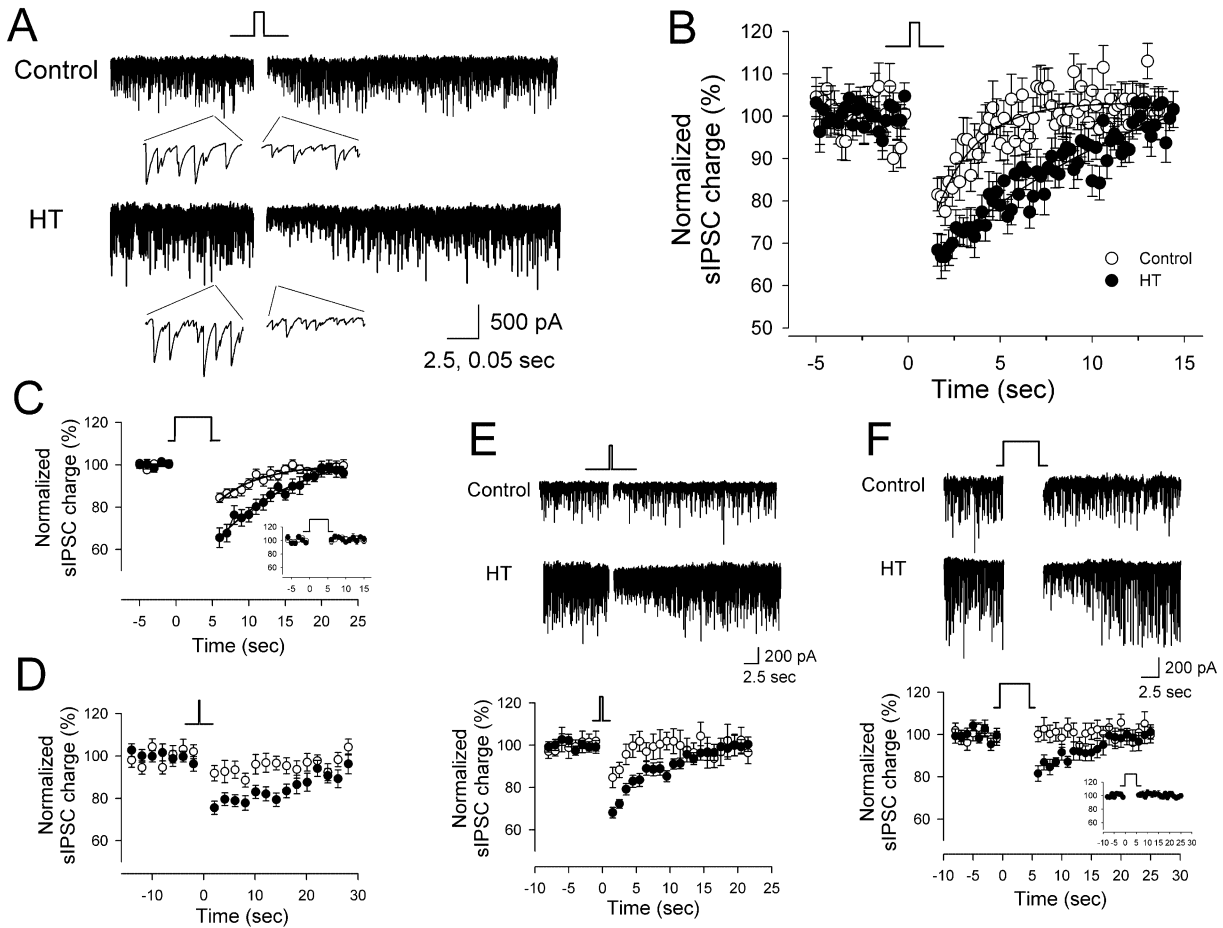


**Figure 1. Long-Term Enhancement of Depolarization-Induced Suppression of Inhibition after Experimental Febrile Seizures**

(A) Current traces from CA1 pyramidal cells from a littermate control (Control) and from an animal that experienced hyperthermia-induced experimental febrile seizures (HT) 1 week before the recording session at postnatal day 10 (the recordings were carried out in the presence of ionotropic glutamate receptor antagonists and carbachol, see text). The spontaneous IPSCs appeared depressed shortly after a depolarizing voltage step (500 ms to 0 mV, indicated by the square pulse above the traces), representing DSI. Note that the depression was more pronounced and longer lasting in the cell from the HT animal.

(B) Combined data from recordings similar to those in (A). The DSI decay was adequately described with a single exponential fit (control, empty circles; HT, filled circles, as in the rest of the figure).

(C) Enhanced DSI was present also when a 5 s long depolarization was used. (Inset) DSI was abolished both in control and HT animals with the CB1 receptor antagonist 1  $\mu$ M SR.

(D) Potentiation of DSI was also present when a short (100 ms) depolarizing pulse was used in the absence of carbachol.

(E) Potentiation of DSI in HT animals was long lasting (5 weeks after seizure induction; depolarizing pulse duration: 500 ms).

(F) Dentate granule cells, which do not normally show DSI in control animals, exhibited significant DSI after the seizures (HT) (depolarizing pulse duration: 5 s). (Inset) SR abolished DSI in dentate granule cells from HT animals.

The frequency of both the action potential-independent miniature IPSCs (mIPSCs, recorded in the presence of the Na channel blocker tetrodotoxin) and the action potential-dependent sIPSCs (recorded in the absence of tetrodotoxin) was reported to be enhanced in a long-term manner in CA1 cells from HT animals (Chen et al., 1999, 2001; Figure 1A). However, the potentiated DSI was not simply a consequence of the presence of higher-frequency sIPSCs, since DSI in HT animals was significantly larger even when the difference in sIPSC activity was eliminated by comparing a subset of control cells with the most intense sIPSC activity with a subset of cells from HT animals with the least intense sIPSC activity (baseline sIPSC charge transfer in this subset of cells from HT animals, expressed as a percent of the

charge transfer in the control group:  $99.0\% \pm 12\%$ ; DSI in these two subsets of cells: control,  $20.4\% \pm 3.4\%$ ,  $n = 8$ ; HT,  $32.4\% \pm 4.3\%$ ,  $n = 8$ ).

The potentiation of DSI could also be observed when long depolarizing current pulses (5 s, instead of the 500 ms used in the previous experiments) were used to evoke DSI (Figure 1C), indicating that the increase in DSI was present with a wide range of depolarizing stimuli (in fact, the potentiation was present even with a 100 ms pulse, see below). DSI was mediated by cannabinoid receptors in both controls and postseizure animals, since the CB1 cannabinoid receptor antagonist SR141716A (SR; 1  $\mu$ M) (Rinaldi-Carmona et al., 1994) abolished DSI in both groups (Figure 1C, inset; DSI in SR in control:  $0.2\% \pm 2.3\%$ ,  $n = 4$ ; HT:  $-3.5\% \pm 2.6\%$ ,

$n = 5$ ; additional experiments showed that 0.005% DMSO, used to dissolve SR, did not change DSI in cells from either control or HT animals. DSI in DMSO in control cells:  $17.0\% \pm 4.0\%$ ,  $n = 3$ ; compared to DSI without DMSO:  $15.6\% \pm 2.2\%$ ,  $n = 6$ ; DSI in DMSO in cells from HT animals:  $35.2\% \pm 7.5\%$ ,  $n = 4$ , compared to without DMSO:  $34.4\% \pm 4.6\%$ ,  $n = 6$ ).

Furthermore, DSI was also larger in cells from HT animals when the experiments were carried out in the absence of carbachol and a short depolarizing pulse (100 ms) was used to evoke DSI (Figure 1D; under these conditions, DSI was small and not significant in controls:  $8.2\% \pm 3.6\%$ ,  $n = 7$ ; but DSI was present in HT:  $24.5\% \pm 3.2\%$ ,  $n = 9$ ). The potentiation of DSI was persistent, since it was still present even 5 weeks after seizure induction (Figure 1E; DSI in control:  $15.3\% \pm 4.8\%$ ,  $n = 10$ ; in HT:  $31.9\% \pm 2.5\%$ ,  $n = 10$ ; note that the enhancement of DSI was unchanged from 1 week to 5 weeks following the seizures, compare Figures 1B and 1E).

In contrast to CA1 pyramidal cells, dentate granule cells have not been shown to exhibit DSI. Although dentate granule cells in control animals did not show DSI (DSI in control:  $-0.1 \pm 3.5$ ,  $n = 10$ ), significant DSI could be observed in these cells 1 week after seizure induction (Figure 1F; DSI in HT:  $18.5\% \pm 3.7\%$ ,  $n = 9$ ; pulse duration in both the control and HT groups: 5 s), indicating that experimental febrile seizures can induce this form of activity-dependent plasticity of the inhibitory system even in cell types that do not typically exhibit DSI. The DSI observed in granule cells from HT animals could be fully blocked by the CB1 receptor antagonist SR (Figure 1F, inset; DSI granule cells from HT animals in SR:  $-0.8\% \pm 3.3\%$ ,  $n = 9$ ).

In the experiments described above, spontaneous IPSCs were used to examine the long-term modifications in DSI after the seizures. As shown in Figure 2A, DSI was also significantly larger when IPSCs were evoked by electrical stimulation (eIPSCs were elicited by an electrode placed near the somatic layer at a constant distance from the recording electrode, as described in Chen et al., 1999; DSI of eIPSCs in controls:  $24.2\% \pm 5.4\%$ ,  $n = 8$ ; in HT:  $40.1\% \pm 5.5\%$ ,  $n = 10$ ; all experiments involving eIPSCs were carried out in the absence of carbachol). Therefore, the potentiation of DSI was present with both spontaneously occurring and stimulation-evoked GABAergic synaptic events. Taken together, these data, obtained with either 100 ms, 500 ms, or 5 s depolarizing pulses, in the presence or absence of carbachol, with sIPSCs or eIPSCs, demonstrate that DSI is significantly potentiated in a long-term manner in principal cells of the hippocampus following a single episode of experimental febrile seizures.

#### Mechanisms of the Persistent Increase in Endocannabinoid Signaling at GABAergic Synapses

Since recent reports indicate that metabotropic glutamate receptor activation increases DSI (Varma et al., 2001), we tested the possibility that the potentiation of DSI took place because of increased tonic metabotropic glutamate receptor (mGluR) activation after the seizures (e.g., resulting from enhanced extracellular glutamate concentration). Prolonged (>30 min) incubation of slices

in the presence of the mGluR antagonist LY341495 (200  $\mu\text{M}$ , a concentration which blocks all mGluRs; Fitzjohn et al., 1998) did not abolish the difference between DSI measured from control and HT animals (DSI in control:  $10.2\% \pm 3.7\%$ ,  $n = 7$ ; in HT:  $24\% \pm 4.8\%$ ,  $n = 8$ ; Figure 2A, inset; note that the mGluR antagonist decreased DSI in both control and HT groups). Muscarinic receptor activation also enhances endocannabinoid release and thus potentiates DSI (Kim et al., 2002). However, tonic increase in acetylcholine levels in the extracellular space could not underlie the observed potentiation of DSI, since DSI in cells from HT animals remained significantly larger compared to controls when slices from both groups were incubated (>45 min) in the presence of the muscarinic receptor antagonist atropine (1  $\mu\text{M}$ ) (DSI in controls:  $15.3\% \pm 4.9\%$ ,  $n = 6$ ; DSI in HT:  $33.9\% \pm 5.0\%$ ,  $n = 6$ ; Figure 2A, inset).

In the experiments described above, the ligands for the CB1 receptors were presumably released from the recorded cells. Therefore, in the next series of experiments we tested the effects of an exogenously applied cannabinoid agonist. WIN55212-2 (WIN; 5  $\mu\text{M}$ ) caused a larger decrease in the amplitude of eIPSCs in cells from HT animals compared to controls and abolished the difference in eIPSCs between the two groups (Figure 2B; in the upper panel, eIPSCs were examined in the same cells before and after switching the perfusate to a solution containing WIN, control:  $n = 10$ , HT:  $n = 10$ ; additional experiments showed that 0.1% DMSO, used to dissolve WIN, had no significant effect on the amplitude of the eIPSCs: change in eIPSC amplitude after switching the perfusate to a medium containing DMSO, with respect to the pre-DMSO baseline:  $2.7\% \pm 6.7\%$ ,  $n = 4$  HT cells; in the lower panel of Figure 2B, the slices were incubated in control medium or in WIN for 40–60 min; control cells without WIN:  $n = 6$ ; control with WIN:  $n = 6$ ; HT without WIN:  $n = 7$ ; HT with WIN:  $n = 7$ ). WIN (5  $\mu\text{M}$ ) had no effect on the eIPSCs in cells from either control or HT animals in the presence of the CB1 antagonist SR (1  $\mu\text{M}$ ; Figure 2C; control cells:  $n = 6$ ; HT:  $n = 6$ ). Furthermore, WIN had a larger effect on eIPSCs in the postseizure animals even 11 weeks after the induction of the seizures (Figure 2D; the slices were incubated in 5  $\mu\text{M}$  WIN for 30–60 min; control without WIN:  $n = 10$ ; control with WIN:  $n = 8$ ; HT without WIN:  $n = 9$ ; HT with WIN:  $n = 5$ ). These findings showed that 5  $\mu\text{M}$  WIN had a significantly larger effect on eIPSCs after the seizures, in agreement with the results obtained with DSI.

CB1 receptor activation with WIN in the hippocampus in normal extracellular medium (i.e., in the absence of elevated levels of extracellular  $\text{K}^+$  and  $\text{Ca}^{2+}$ ) typically does not alter the frequency or amplitude of mIPSCs (Hoffman and Lupica, 2000). The mIPSC frequency was previously shown to be persistently enhanced after experimental complex febrile seizures, without a change in mIPSC amplitude (Chen et al., 1999). The elevated frequency of the mIPSCs after the seizure induction remained insensitive to CB1 receptor activation (note that the elevated mIPSC frequency was also insensitive to blockade of voltage-gated  $\text{Ca}^{2+}$  channels; Chen et al., 1999). Specifically, the frequency of mIPSCs in cells from HT animals remained increased in the presence of WIN (5  $\mu\text{M}$ ), since the agonist had no significant effect on the frequency or the amplitude of the mIPSCs in

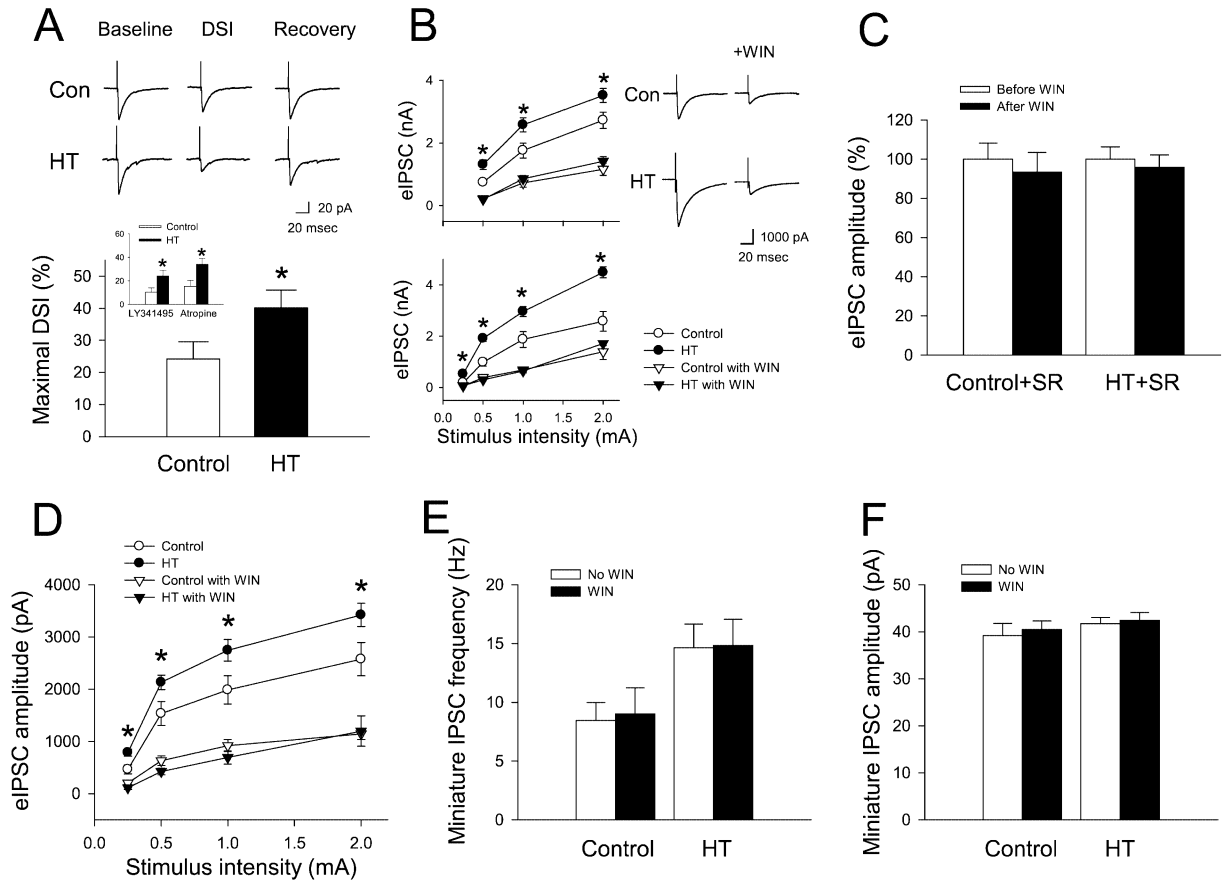


**Figure 2.** Persistent Increase in DSI of Evoked IPSCs, and Effects of Exogenously Applied Cannabinoid Agonist

(A) The enhancement of DSI (1 week after seizure induction) was present not only with spontaneous IPSCs in carbachol (Figure 1) but also with evoked IPSCs without carbachol (depolarizing pulse: 5 s). (Inset) DSI remained enhanced after the seizures (HT) in the presence of the metabotropic glutamate receptor antagonist LY341495 or the muscarinic receptor blocker atropine.

(B) The cannabinoid agonist WIN (5  $\mu$ M) depressed the eIPSCs to a greater extent in cells from HT animals, both when the agonist was washed in following a period of pre-drug recording (upper panels) and when the slices were incubated either with or without the agonist (bottom panel).

(C) In the presence of the CB1 antagonist SR (1  $\mu$ M), switching the perfusate to WIN (5  $\mu$ M) had no effect on the eIPSCs in cells from either control or HT animals.

(D) The CB1 agonist had a larger effect on eIPSCs, even 11 weeks after the seizure episode.

(E and F) The CB1 agonist had no effect on the frequency (E) or amplitude (F) of miniature IPSCs (note that the frequency of mIPSCs is enhanced in HT animals, Chen et al., 1999).

either the control or the postseizure group (Figures 2E and 2F; control without WIN:  $n = 15$ ; control with WIN:  $n = 14$ ; HT without WIN:  $n = 15$ ; HT with WIN:  $n = 13$ ; the slices were incubated in 5  $\mu$ M WIN for 25–50 min; 1 week after seizures).

The results obtained with the exogenous application of the CB1 receptor agonist WIN indicate that the long-lasting potentiation of DSI in CA1 pyramidal cells after hyperthermia-induced seizures is likely to involve a presynaptic locus, since an exclusively postsynaptic mechanism alone, e.g., enhanced release of endocannabinoid ligands in response to the same amount of depolarization, cannot explain the fact that exogenous application of WIN had a larger effect on the eIPSCs after the seizures compared to controls. Moreover, the lack of sensitivity of the mIPSCs to cannabinoid receptor activation in cells from animals that had experimental febrile sei-

zures also indicates that this putative presynaptic mechanism underlying the enhanced endocannabinoid-mediated retrograde signaling following the seizures is specific to action potential-dependent GABA release.

In order to determine the nature of the presynaptic mechanisms that may be involved in the long-term plasticity of DSI, the effect of the CB1 receptor antagonist SR (1  $\mu$ M) was tested on eIPSCs. In agreement with previous reports, SR had no effect on the eIPSCs in controls (Hoffman and Lupica, 2000; Wilson and Nicoll, 2001). However, SR caused a significant increase in the eIPSCs after the seizures (Figure 3A; for the results in the lower panel, the slices were incubated either without or with SR for >30 min; control without SR:  $n = 6$ ; control with SR:  $n = 7$ ; HT without SR:  $n = 7$ ; HT with SR:  $n = 7$ ; similar results were obtained when the perfusate was switched to SR during recordings from the same cells,

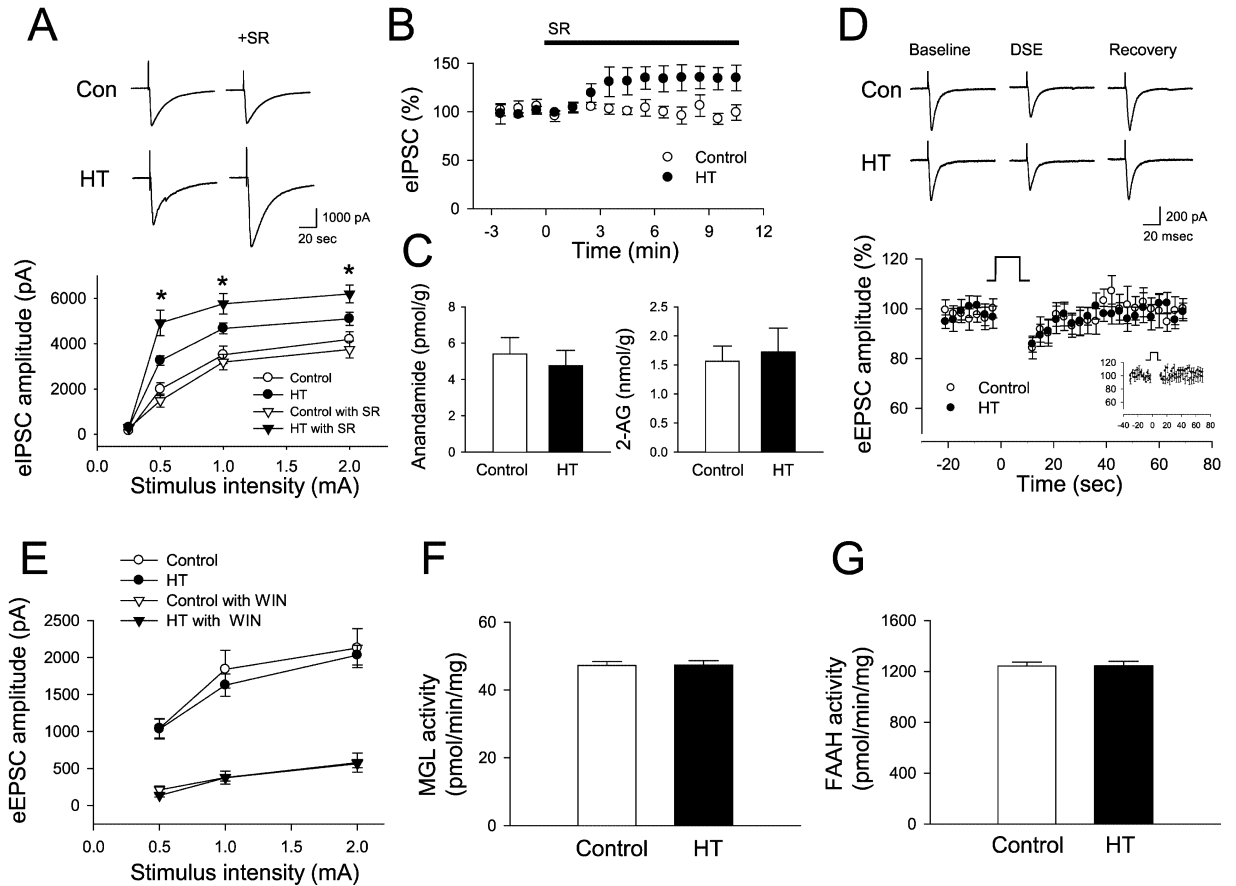


Figure 3. Specificity of Seizure-Induced Alterations in Endocannabinoid Signaling

(A) The CB1 receptor antagonist SR (1 μM) had no significant effect on eIPSCs in controls; however, it caused an increase in the peak amplitude of the eIPSCs in cells from animals that experienced seizures 1 week before (HT).  
 (B) Time course of the SR effect on eIPSCs.  
 (C) HPLC experiments indicate that the concentrations of anandamide and 2-AG did not change in the hippocampus after the seizures.  
 (D) In spite of the marked changes in DSI, DSE was not altered by the seizures (depolarizing step: 10 s). (Inset) SR (1 μM) abolished DSE in both control and postseizure animals.  
 (E) In agreement with the lack of alteration in DSE, the CB1 agonist WIN (5 μM) caused similar changes in the eEPSCs in cells from control and HT animals.  
 (F and G) Enzyme activity assays showed lack of seizure-induced alterations in cannabinoid breakdown for either monoglycerol lipase (MGL, in [F]) or for fatty acid amino hydrolase (FAAH, in [G]).

as shown in Figure 3A, upper panel; enhancement of the eIPSC amplitude by SR in cells from HT animals:  $35\% \pm 17\%$ ,  $n = 10$ , with respect to the pre-SR baseline). The time course of the SR effect on eIPSCs, indicating saturation of the SR-induced enhancement of the eIPSCs in cells from HT animals, is shown in Figure 3B (SR effect measured 5–10 min after switching the perfusate to SR, expressed as percent of pre-SR baseline, in control:  $99.7\% \pm 3.2\%$ ,  $n = 5$ ; HT:  $134.7\% \pm 4.7\%$ ,  $n = 6$ ; note that the data in Figure 3B are from a different set of cells than in Figure 3A, since in the time course experiments only a single stimulation intensity was used in order to monitor the development of the SR action).

One possible explanation for the amplitude-enhancing effect of the CB1 antagonist on the eIPSCs after the seizures is that there is a tonic activation of CB1 receptors due to increased steady-state levels of the

endocannabinoid ligands. Although this mechanism was unlikely, given both the more intense sIPSC activity and the potentiated eIPSCs in cells from HT animals, experiments were carried out to measure the steady-state levels of endocannabinoids in the hippocampi of control and HT animals. High-performance liquid chromatography/mass spectrometry (HPLC/MS) analyses (Giuffrida et al., 2000; Dinh et al., 2002) revealed no significant change in the concentrations of either anandamide or 2-AG in the hippocampus of HT animals (Figure 3C; anandamide, in pmol/g hippocampal tissue, controls:  $5.40 \pm 0.89$ ,  $n = 4$ ; HT:  $4.75 \pm 0.83$ ,  $n = 4$ ; 2-AG, in nmol/g hippocampal tissue, controls:  $1.56 \pm 0.26$ ,  $n = 4$ ; HT:  $1.72 \pm 0.41$ ,  $n = 4$ ; 1 week after seizure induction). Although the HPLC/MS assay could not determine the ligand concentration selectively in the extracellular space, these data indicated the lack of a large, sustained change in the total levels of endocannabinoids in the

postseizure tissue (additional evidence arguing against alterations in endocannabinoid release came from the DSE experiments described below).

### **Potential of the Endocannabinoid-Mediated Retrograde Signaling System Is Specific to Inhibitory Synapses**

It has been reported recently that activity-dependent release of endocannabinoids can depress transmitter release not only from GABAergic axons but also from glutamatergic terminals (Ohno-Shosaku et al., 2002). Although it is not yet clear whether a different endocannabinoid acts on CB receptors on inhibitory versus excitatory terminals and/or whether a novel CB-like receptor exists on GABAergic versus glutamatergic axons (Hájos and Freund, 2002), DSE offers a possibility to examine whether the enhanced amplitude and prolonged decay of the suppression of transmitter release by endocannabinoids after experimental complex febrile seizures is specific to inhibitory terminals. As shown in Figure 3D, DSE was identical in CA1 cells from control and postseizure animals (1 week after the seizures; DSE in controls:  $15.8\% \pm 4.2\%$ ,  $n = 8$ ; in HT:  $14.2\% \pm 3.2\%$ ,  $n = 8$ ; DSE was evoked using a 10 s long pulse; Ohno-Shosaku et al., 2002), indicating that there is no overall increase in the endocannabinoid-mediated retrograde signaling system involving both the excitatory and inhibitory terminals. The selective enhancement of DSI but not DSE is also consistent with the results described above that indicate that the potentiation of DSI has a presynaptic locus and that it is not due to a postsynaptic mechanism such as increased release of endocannabinoids from the pyramidal cells. The DSE in cells from both control (Ohno-Shosaku et al., 2002) and postseizure animals could be abolished by the CB1 receptor antagonist SR (1  $\mu\text{M}$ ) (Figure 3D, inset; DSE with SR: control:  $6.9\% \pm 5\%$ ,  $n = 7$ ; HT:  $5.8\% \pm 5.3\%$ ,  $n = 7$ ; the effect of SR on DSE was significant). In agreement with the lack of alterations in DSE and in contrast to the larger effect of 5  $\mu\text{M}$  WIN on eIPSCs from HT animals (Figure 2B), WIN (5  $\mu\text{M}$ ) did not cause a differential change in eEPSCs in cells from control and postseizure animals (1 week after seizures; Figure 3E;  $n = 8$  cells in all four groups).

### **Lack of Changes in the Endogenous Cannabinoid-Inactivating Systems**

Alterations in the uptake of endogenously released cannabinoids may contribute to the changes in DSI after the seizures, particularly to the prolonged DSI decay in HT animals. However, experiments with AM-404 (20  $\mu\text{M}$ ), an inhibitor of the anandamide/2-AG transporter (Beltramo et al., 1997), showed that blockade of endocannabinoid uptake did not prolong the decay of the DSI in either the control (in agreement with previous reports, Wilson and Nicoll, 2001) or the HT groups (DSI decay time constants: control, before AM-404, 5.9 s; after AM-404, 4.5 s,  $n = 6$ ; HT, before AM-404, 12.5 s; after AM-404, 11.1 s,  $n = 6$ ; the perfusate was switched from a control solution to a medium containing AM-404 for 10–15 min; DSI was evoked using 5 s depolarizing pulses, in the presence of carbachol; 1 week postseizure; data not shown). These findings indicated that the

slower kinetics of the DSI decay after the seizures was not due to an AM-404-blockable uptake system. These results were in agreement with our endocannabinoid measurements, indicating that the steady-state levels of endocannabinoids remained unchanged. As reported before (Wilson and Nicoll, 2001), AM-404 also decreased the amplitude of DSI (perhaps due to occlusion of DSI following the blockade of endocannabinoid uptake; Wilson and Nicoll, 2001), in both controls and postseizure animals (decrease in DSI in AM-404 after 10–15 min perfusion, with respect to the pre-AM-404 DSI: control,  $37.9\% \pm 20.2\%$ ,  $n = 5$ ; HT,  $49.4\% \pm 19.1\%$ ,  $n = 5$ ; difference is not significant; data not shown), indicating that AM-404 reached the recorded cell, and therefore, the lack of an effect of AM-404 on the DSI decay was not due to a lack of penetration of the drug into the slice.

The larger amplitude and longer decay of DSI following experimental complex febrile seizures could also take place if the activity of the enzymes that inactivate the endocannabinoids was reduced following the seizures. However, enzyme activity assays for monoacylglycerol lipase (MGL) (Dinh et al., 2002) and fatty acid amide hydrolase (FAAH) (Desarnaud et al., 1995; Cravatt et al., 1996) in the hippocampus did not reveal any significant alteration between control and postseizure groups (Figures 3F and 3G; MGL activity, in pmol/min/mg protein: control,  $47.2 \pm 1.1$ ,  $n = 6$ ; HT,  $47.3 \pm 1.3$ ;  $n = 5$ ; FAAH: control,  $1242.5 \pm 29.9$ ,  $n = 6$ ; HT,  $1244.7 \pm 35.2$ ,  $n = 5$ ). Together, these results indicated that changes in endocannabinoid-inactivating systems were unlikely to underlie the persistent potentiation of DSI after seizures.

### **Unchanged Site Specificity of Expression but Increased Numbers of CB1 Receptors following Experimental Febrile Seizures**

The electrophysiological data on the enhanced effects of the exogenously applied cannabinoid agonist on eIPSCs in cells from HT animals, together with a lack of significant alterations in endocannabinoid levels, were consistent with a presynaptic locus for the observed long-term plasticity of DSI. Therefore, we tested the hypothesis that the expression levels of presynaptic CB1 receptors changed following the seizures. Double-labeling experiments showed that immunoreactivity for CB1 receptors was localized specifically to CCK-positive cells and axons (Figures 4A and 4B) but not to parvalbumin (PV)-positive processes (Figures 4C and 4D), both in controls (data not shown; Katona et al., 1999; Tsou et al., 1999) and after experimental complex febrile seizures (Figures 4A–4D; number of CCK-labeled axon-like processes double labeled for CB1 receptors: control, 179/183, i.e., 97.7% of CCK-containing processes were also positive for CB1 receptors,  $n = 3$  animals; HT, 159/165, 96.4%,  $n = 3$ ; number of PV-labeled presumed axons double labeled for CB1 receptors: control, 0/252, 0%,  $n = 4$ ; HT, 0/264, 0%,  $n = 4$ ). These findings indicated that the high specificity of CB1 receptor expression in hippocampal interneurons (Katona et al., 1999; Tsou et al., 1999; Wilson et al., 2001) was preserved after the experimental complex febrile seizures. The characteristic layer-specific pattern of

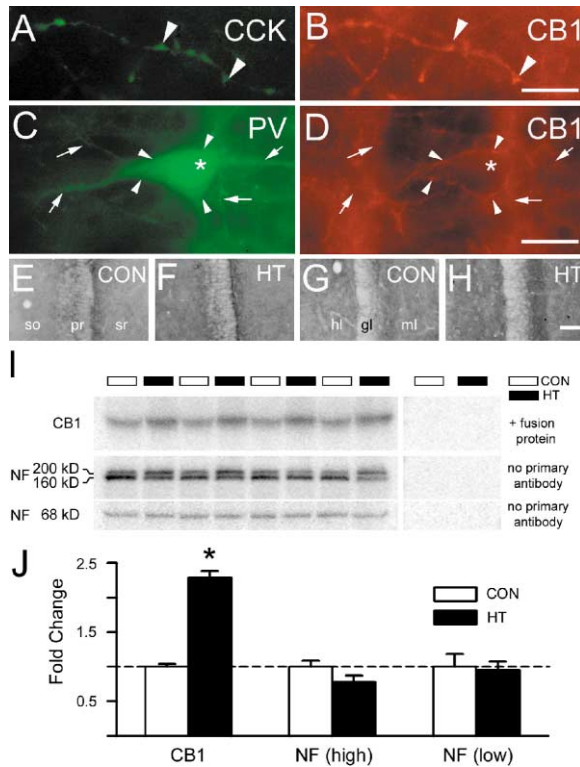


Figure 4. Increased Number of CB1 Receptors after Experimental Febrile Seizures

(A–D) Similar to littermate control animals (data not shown; Katona et al., 1999), CB1 receptors after the seizures (A–D) remained localized to CCK+ processes (A and B), whereas PV+ processes (arrows) remained CB1 negative (C and D). Note that the CB1+ axon terminals indicated by arrowheads in (B) surround the PV+, CB1-negative interneuron indicated by the asterisk.

(E–H) The characteristic layer-specific pattern of CB1 receptor staining was unchanged after the seizures, both in CA1 (E and F) and dentate gyrus (G and H), but the staining intensity appeared stronger after the seizures (so, stratum oriens; pr, stratum pyramidale; sr, stratum radiatum; hl, hilus; gl, granule cell layer; ml, molecular layer). (I and J) Western blots (I) (performed on hippocampal tissue) and their quantitative analysis (J) show the over 2-fold increase in CB1 receptors after the seizures (HT) compared to littermate controls (CON), without changes in control proteins (NF, neurofilament; NF (high), 200 kDa and 160 kDa; NF (low), 68 kDa in [G]). The right-hand panel in (I) illustrates the lack of detectable proteins with antibody preincubated with fusion protein and in the no primary antibody control blots. Each lane in (I) represents a different animal (note the consistently enhanced quantity of CB1 receptors in each of the HT animals in the blots in [I]). Scale bars, 10  $\mu$ m (A and B); 20  $\mu$ m (C and D); 50  $\mu$ m (E–H).

CB1 receptor staining (Katona et al., 1999) was unchanged after the seizures, both in the CA1 (Figures 4E and 4F) and the dentate gyrus (Figures 4G and 4H), but the staining intensity qualitatively appeared stronger in animals that experienced seizures. Quantitative Western blot analyses demonstrated a significant increase in CB1 receptor protein in hippocampi from animals that experienced seizures, compared to controls (Figures 4I and 4J), without alterations in the amount of control proteins (all values represent fold changes, normalized to mean control values: CB1 receptor: control:  $1.0 \pm 0.04$ ; HT:  $2.28 \pm 0.1$ ; control proteins: neurofilament

high: control:  $1.0 \pm 0.08$ ; HT:  $0.771 \pm 0.1$ ; neurofilament low: control:  $1.0 \pm 0.181$ ; HT:  $0.95 \pm 0.12$ ;  $n = 4$  animals in both groups). These Western blotting results show a significant upregulation of CB1 receptors in the hippocampus after complex febrile seizures.

#### Potential of DSI of Cannabinoid-Sensitive Single-Fiber Responses

What is the relationship between the increased DSI and the enhanced CB1 receptor number? The increased DSI in the experiments carried out on sIPSCs (Figure 1) or multifiber eIPSCs (Figures 2A and 2B) could have originated simply from a relative potentiation of the GABA responses originating from CB1 receptor-containing axons, without an involvement of the increased CB1 receptor number. In order to examine this question, minimal stimulation-evoked, presumed unitary, single-fiber IPSCs (meIPSCs; Figures 5A and 5B) were examined in slices incubated in 250 nM  $\omega$ -agatoxin TK, a P/Q-type voltage-dependent  $Ca^{2+}$  channel antagonist which has been shown to block the GABA release from perisomatic fibers that are not sensitive to cannabinoids (Wilson et al., 2001). The meIPSCs recorded under these conditions from CA1 cells from HT animals were larger compared to controls (Figure 5C; control:  $67.0 \pm 6$  pA,  $n = 17$ ; HT:  $90.0 \pm 8$  pA,  $n = 24$ ; rise time constants: control:  $0.67 \pm 0.06$  ms; HT:  $0.69 \pm 0.07$  ms). As shown in Figures 5D and 5E, DSI was significantly enhanced after the seizures (DSI following a 1 s long depolarizing pulse in control:  $45\% \pm 13\%$ ,  $n = 8$ ; in HT:  $76\% \pm 6\%$ ,  $n = 16$ ; note that all unitary responses tested under these conditions exhibited DSI, in agreement with Wilson et al., 2001). In five cells in each group, the effect of WIN was also tested on the meIPSCs. In each case, WIN (5  $\mu$ M) completely abolished the meIPSCs (Figures 5D and 5E), indicating that the lack of a complete (100%) DSI following a 1 s depolarizing pulse was not due to the involvement of a cannabinoid-insensitive component (note that there was no difference in the time course of the WIN effect on the meIPSCs from cells in control and HT animals; Figure 5F). The enhanced meIPSCs recorded from slices incubated in  $\omega$ -agatoxin TK suggest that the potentiation of DSI of the sIPSCs and the multifiber eIPSCs was, at least in part, due to a relative increase of the GABA responses originating from the CB1-containing axons. These results are consistent with the observation that WIN abolished the difference between the eIPSCs from control and HT animals (Figure 2B). However, the fact that DSI was enhanced in cells from HT animals even when the DSI-susceptible unitary responses were examined in isolation in the minimal stimulation experiments indicates that the increase in the number of CB1 receptors enhances the sensitivity of the axon terminals to endocannabinoids and, therefore, contributes to the observed increase in DSI of sIPSCs and eIPSCs.

#### Lack of Sprouting of CB1-Containing Axons

Next, we examined whether the increased number of CB1 receptors and the enhancement of the DSI-susceptible responses (Figure 5C) were due to an increase in the number of synapses made by CB1-containing axons on CA1 pyramidal cell somata. Quantitative electron mi-



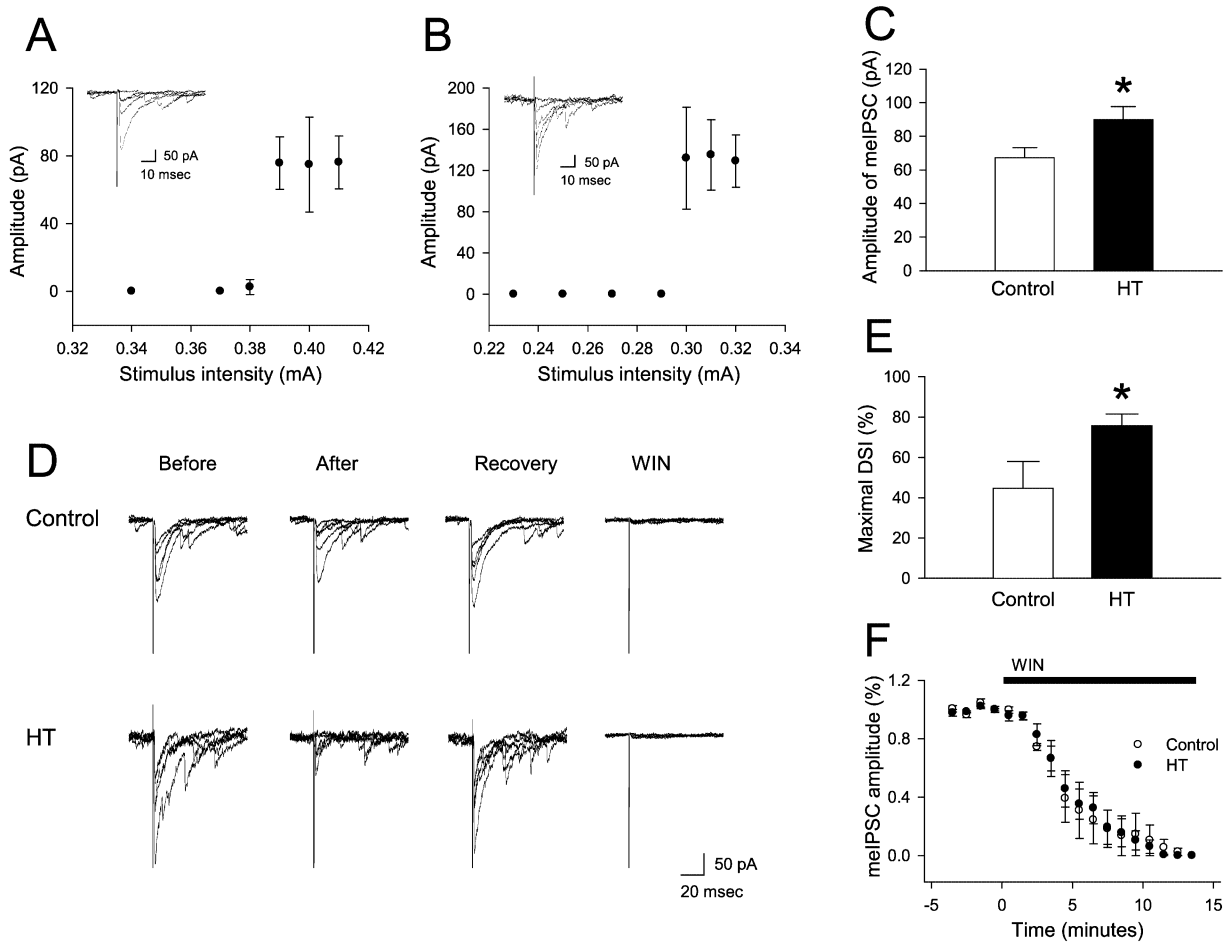


Figure 5. Potentiated DSI of Single-Fiber IPSCs

(A and B) Minimal stimulation-evoked IPSCs (meIPSCs) from a CA1 cell from a control (A) and an HT (B) animal exhibit a sharp, stepwise increase in peak amplitude with increasing stimulation intensity, indicating the successful isolation of a single fiber.

(C) Summary data show that the meIPSCs were larger after the seizures (1 week following seizure induction; all recordings were in slices incubated in  $\omega$ -agatoxin TK).

(D) The DSI of meIPSCs was significantly enhanced after the seizures (meIPSCs are shown before and after the 1 s depolarizing pulse). WIN (5  $\mu$ M) invariably abolished the meIPSCs, indicating that the lack of a complete (100%) DSI following a 1 s depolarizing pulse was not due to the involvement of a cannabinoid-insensitive component.

(E) Summary data of the DSI of the meIPSCs.

(F) There was no difference in the time course of the WIN effect on meIPSCs between the two groups.

croscopy, based on the dissector sampling method that is not sensitive to changes in the size of the examined objects (West, 1999; see legend to Figures 6D and 6E and Experimental Procedures), showed no significant seizure-induced increases in the number of CB1-immunoreactive synapses on pyramidal cell bodies (Figures 6A–6E and 6J; synapse density: control,  $10.2 \pm 0.9$  per  $10^3 \mu\text{m}^3$ ,  $n = 145$  synapses from  $n = 3$  animals; HT,  $12.2 \pm 0.7$  per  $10^3 \mu\text{m}^3$ ,  $n = 160$  synapses from  $n = 3$  animals). Similarly to the identified CB1-positive synapses, there was also no significant increase in the number of transected CB1-immunostained axonal profiles (including synaptic terminals, as well as terminals that in the examined section did not make synapses, and interterminal axon segments; see arrows in Figures 6A and 6B) per unit area within the CA1 pyramidal cell layer (Figure 6K; control:  $30.0 \pm 2.2$  profiles per  $10^3 \mu\text{m}^2$ ,  $n = 1020$ ; HT:  $33.7 \pm 2.7$  profiles per  $10^3 \mu\text{m}^2$ ,  $n = 1042$ ).

These electron microscopic results were independently corroborated using a different approach based on preembedding immunogold staining of CB1-containing processes (see Experimental Procedures and Figures 6F–6I; the major advantage of the technique is that tens of thousands of profiles can be sampled, which is not practical with electron microscopy). Again, there was no evidence of sprouting of the CB1-positive axons in either the pyramidal cell layer (Figure 6L; control:  $34.3 \pm 1.0$  profiles per  $10^3 \mu\text{m}^2$ ,  $n = 10,310$ ; from  $n = 3$  animals; HT:  $31.9 \pm 0.9$  profiles per  $10^3 \mu\text{m}^2$ ,  $n = 11,615$ ; from  $n = 3$  animals) or in the stratum radiatum (Figure 6M; control:  $54.3 \pm 1.7$  profiles per  $10^3 \mu\text{m}^2$ ,  $n = 12,706$ ; HT:  $50.2 \pm 1.5$  profiles per  $10^3 \mu\text{m}^2$ ,  $n = 13,005$ ). Note that an internal control for the validity of the light microscopic sampling based on the preembedding immunogold technique was the fact that the profile density obtained with the electron microscopic sampling was similar to

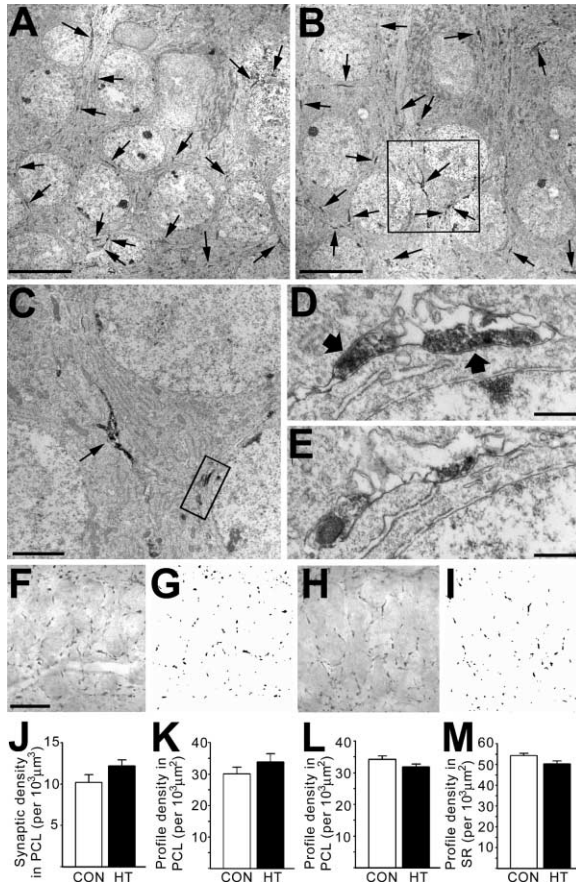


Figure 6. Lack of Sprouting of CB1-Positive Axons after the Seizures

(A and B) Low-power electron micrographs of the stratum pyramidale are shown from control (A) and HT animals (B). Transected, immunolabeled profiles (including terminals and interterminal axon segments) are indicated by arrows.

(C) The framed area in (B) is shown at a higher magnification.

(D and E) Illustration of the disector method. The framed area in (C) at even higher magnification in (D) reveals the presence of two perisomatic CB1-positive synapses. In (E), the image of the same area as in (D) three sections (210 nm) away shows the absence of synapses. With the disector method, only those synapses were counted which were present in the first but not in the fourth section. Thus, both of the synapses in (D) were counted, since they were not present in (E).

(F–I) Light microscopic images of the preembedding CB1 receptor immunogold staining from control (F) and HT (H) animals show the immunopositive axons in stratum pyramidale. The background of the grayscale images (F and H) was subtracted using high-pass filtering, resulting in corresponding binary images ([G] for [F] and [I] for [H]) where the number of the immunostained axonal profiles could be counted.

(J–M) Quantitative data from the electron microscopic measurement of the density of CB1+ synapses (J) and axonal profiles ([K]; see arrows in [A] and [B]) in the pyramidal cell layer (PCL). The CB1+ axonal profile density from the immunogold experiments was determined for both the pyramidal cell layer (L) and the stratum radiatum (M; SR, stratum radiatum). Note that the profile densities obtained with electron microscopy (K) and with the immunogold technique (L) were similar.

Scale bars, 10  $\mu\text{m}$  (A and B); 5  $\mu\text{m}$  (C); 1  $\mu\text{m}$  (D and E); 20  $\mu\text{m}$  (F).

the data from the preembedding immunogold method (compare the data in Figure 6K with Figure 6L). Taken together, these data showed that the mechanism underlying the enhanced mIPSCs peak amplitude and the increase in CB1 receptor numbers per unit weight of hippocampal tissue (Figures 4I and 4J) was not sprouting of CB1/CCK-positive axons. Since there was no significant sprouting, the increase in the CB1 receptor density detected using Western blots most likely reflected an increase in the number of CB1-positive receptors on the axon terminals of CCK-positive interneurons, in agreement with the electrophysiological data.

## Discussion

Experimental prolonged, complex febrile seizures result in a long-term, PKA-dependent, presynaptic potentiation of perisomatic, GABA<sub>A</sub> receptor-mediated IPSCs in CA1 pyramidal cells (Chen et al., 1999), and they also persistently modify intrinsic membrane currents such as  $I_h$  in the postsynaptic membrane (Chen et al., 2001). Here we demonstrate that febrile seizures lead to long-term alterations in the endocannabinoid-mediated, retrograde signaling at perisomatic GABAergic synapses. The data in this paper support the general conclusion of our previous studies that a single episode of prolonged febrile seizures (which are the type of febrile seizures that are most consistently associated with subsequent temporal lobe epilepsy; Shinnar, 1998) in the hyperthermia model in rats causes long-lasting changes in neuronal excitability in the limbic system (for reviews on the effects of early life seizures, see Holmes and Ben-Ari, 1998; Walker and Kullmann, 1999).

To our knowledge, the data show for the first time that the activity-dependent, CB1 receptor-mediated depression of GABA release can undergo persistent alterations. Long-term plasticity in the gain of retrograde, endocannabinoid-mediated signaling could result from postsynaptic (e.g., changes in endocannabinoid release) or presynaptic factors (Varma et al., 2002), and/or modifications in endocannabinoid-inactivating systems. Out of these potential regulatory sites, our data point to an increase in CB1 receptors on CCK-positive interneuronal axon terminals, many of which make perisomatic synapses on hippocampal principal cells. The postseizure increase in CB1 receptor expression was indicated by the Western blot experiments and was consistent with the enhanced DSI amplitude. The seizure-induced alterations in CB1 signaling were strong enough to convert a population of principal cells, the dentate granule cells that do not normally express DSI, to exhibit robust DSI, indicating an enhanced role for endocannabinoids in regulating neuronal excitability levels within the postseizure limbic networks.

Since sIPSCs and eIPSCs constitute mixed responses that include both cannabinoid-sensitive and -insensitive components, a selective increase in the amplitude of the cannabinoid-sensitive IPSCs alone could also enhance the DSI of sIPSCs and eIPSCs, irrespective of alterations in CB1 receptor numbers. Indeed, WIN in the experiments in Figure 2B abolished the difference between the eIPSCs in cells from control and HT animals, indicating that a selective potentiation of the can-

nabinoid-sensitive synaptic inputs took place after the seizure induction. Consistent with these data, the mEPSC amplitude in  $\omega$ -agatoxin TK was significantly increased (Figure 5C). While a selective potentiation of the IPSCs evoked by GABA from CB1 receptor-containing fibers may contribute to the increased DSI of sIPSCs and eIPSCs, it cannot explain the fact that DSI was enhanced even in the case of the single-fiber mEPSCs in  $\omega$ -agatoxin TK (Figure 5E), i.e., under conditions when only the DSI-susceptible inputs were studied. Therefore, the potentiation of DSI of the mEPSCs in  $\omega$ -agatoxin TK indicates that the increased number of CB1 receptors constitutes a major mechanism underlying the potentiation of the endocannabinoid-mediated, activity-dependent inhibition of GABA release after the seizures.

The long-term modification in the endocannabinoid signaling was not restricted to potentiation of peak DSI, since it also included the ability of the CB1 antagonist to enhance the amplitude of eIPSCs in the postseizure neurons but not in control cells. A proportion of the CB1 receptors has been suggested to exist in a constitutively active state (i.e., active without a ligand) that depresses transmitter release, and the CB1 receptor antagonist SR has been proposed to act as an inverse agonist at these receptors to reverse the constitutive activity (Bouaboula et al., 1997; Pan et al., 1998; Vasquez and Lewis, 1999). In the hippocampi of control animals, SR causes no significant enhancement of GABA release (Hoffman and Lupica, 2000; Wilson and Nicoll, 2001). However, an increase in the number of CB1 receptors after the seizures is expected to also enhance the number of constitutively active CB1 receptors (Vasquez and Lewis, 1999), which should result in a greater effect of SR on eIPSCs, as observed in HT animals. Therefore, the sensitivity of the eIPSCs to the CB1 antagonist after the seizures is consistent with enhanced expression levels for CB1 receptors. The elevation of the number of CB1 receptors per perisomatic basket cell synaptic terminal was also indicated by the fact that the increase in the CB1 receptor expression (shown by the Western blots) took place without an increase in the density of CB-positive synapses and axonal profiles in the pyramidal cell layer following the seizures.

In addition to the enhanced peak DSI and the increased sensitivity of IPSCs to the CB1 antagonist, the third type of seizure-induced alteration in the cannabinoid signaling system was the dramatic prolongation of DSI decay. The slower DSI decay was not caused by a decrease in an AM-404-blockable uptake system, since AM-404 did not change the decay time constant of DSI in either control (consistent with Wilson and Nicoll, 2001) or HT animals. The prolongation of DSI was also not due to significant alterations in the endocannabinoid-inactivating enzymatic systems, since the activity levels of either FAAH (Egertová et al., 1998) or MGL (Dinh et al., 2002) did not change. On the other hand, alterations in the expression levels of proteins related to G protein signaling can modulate the time course of G protein signals (Chen and Lambert, 2000); therefore, it is possible that the prolongation of DSI decay is also related to the augmented levels of CB1 receptor expression after the seizures.

The increase in CB1 receptors occurred selectively

only on those interneurons which normally express these receptors, i.e., on the CCK-positive basket cells, because no CB1 receptor expression could be observed on parvalbumin-positive interneurons either in controls or in HT animals (CCK- or parvalbumin-containing interneurons together make up the total basket cell population, Freund and Buzsáki, 1996; experimental febrile seizures do not lead to hippocampal cell loss, Toth et al., 1998). The seizure-induced enhancement in cannabinoid signaling was selective also in terms of affecting GABAergic but not glutamatergic terminals, since only DSI, but not DSE, showed significant alterations following the seizures.

GABAergic transmission is involved in a diverse array of functional roles (McBain and Fisahn, 2001), and the data in this paper show that, in addition to pre- and postsynaptic plasticity mechanisms (Nusser et al., 1998; Brooks-Kayal et al., 1998; Chen et al., 1999, 2001; Chevaleyre and Castillo, 2003), the endocannabinoid-mediated retrograde regulation of GABA release can also undergo long-term modification in the central nervous system. To our knowledge, the persistent potentiation of DSI following febrile seizures constitutes the first demonstration of robust modifications in cannabinoid receptor function in a clinically relevant brain disorder. Although the question of whether normal patterns of neuronal firing are sufficient to evoke substantial DSI is currently debated (Hampson et al., 2003), intense epileptiform burst firing has been shown to trigger DSI, in the form of decreased IPSPs following each seizure-like event (Beau and Alger, 1998). The precise roles of the various endocannabinoids in the modulation of seizure thresholds are likely to be complex (Ameri et al., 1999; Wallace et al., 2002; Clement et al., 2003), since both GABAergic and glutamatergic terminals on both principal cells and interneurons can contain CB-type receptors, some with unusual pharmacological profiles (Hájos and Freund, 2002). However, the high specificity of the seizure-induced alterations in CB1 receptor-mediated signaling described here indicates that the endocannabinoid system may provide novel targets for therapeutic drug development (Piomelli et al., 2000; Kathuria et al., 2003) to control seizures in epilepsy.

## Experimental Procedures

### Hyperthermia-Induced Seizures

The hyperthermia-induced seizure paradigm has been described elsewhere (Chen et al., 1999, 2001). In brief, on postnatal day 10, the core temperature of pups was raised using a regulated stream of moderately heated air. Rectal temperatures were measured at baseline, at 2 min intervals, and at the onset of hyperthermic seizures, which occur in virtually all rats. Hyperthermia (defined as core temperature  $>39.5^{\circ}\text{C}$ ) was maintained for 30 min, aiming for a core temperature of  $41^{\circ}\text{C}$ – $42^{\circ}\text{C}$ , and the presence and duration of seizures for each pup were noted at 2 min intervals. Seizure duration in this model has been shown to average 22 min, and threshold temperature to seizure onset averaged  $41.1^{\circ}\text{C}$ . Following the hyperthermia period, rats were placed on a cool surface, monitored for 15 min, and then returned to home cages.

### Slice Preparation

Control and experimental littermate Sprague-Dawley rats (Zivic-Miller, Zelienople, PA) were anesthetized with halothane 1–11 weeks after seizure induction, decapitated, and their brains removed. Brain slices were prepared (Chen et al., 1999) in artificial cerebrospinal

fluid (ACSF) composed of 126 mM NaCl, 2.5 mM KCl, 26 mM NaHCO<sub>3</sub>, 2 mM CaCl<sub>2</sub>, 2 mM MgCl<sub>2</sub>, 1.25 mM NaH<sub>2</sub>PO<sub>4</sub>, and 10 mM glucose.

#### Electrophysiology

Blind whole-cell recordings were obtained in an interface-type chamber at 35°C, using an Axopatch-200A amplifier (Axon Instruments, Foster City, CA). Spontaneous IPSCs were recorded in ACSF containing 10 μM D-2-amino-5-phosphovaleric acid (APV; Tocris), 5 μM 6-cyano-7-nitroquinoxaline-2,3-dione (CNQX; Tocris), and unless specifically indicated, 5 μM carbachol (Sigma). For miniature IPSCs, the ACSF contained 10 μM APV, 5 μM CNQX, and 1 μM tetrodotoxin (TTX; Calbiochem). To evoke perisomatic IPSCs (latency <3.1 ms), constant-current stimuli (20 μs) were applied through a bipolar 90 μm tungsten electrode. The placement and distance of the recording and stimulating electrodes were kept constant as described (Chen et al., 1999). For minimal stimulation, a patch pipette was used as a stimulating electrode. Pipette solutions for DSI experiments consisted of 140 mM CsCl, 2 mM MgCl<sub>2</sub>, 10 mM N-2-hydroxyethylpiperazine-N-2-ethanesulfonic acid (HEPES), 3 mM QX-314, 0.2 mM EGTA, 1 mM ATP, and 0.2 mM GTP (for eIPSCs, no EGTA, ATP, or GTP was included in the pipette; for DSE, CsCl was replaced with K-gluconate). The depolarizing pulse used to evoke DSI was a 100 ms to 5 s step to 0 mV from holding potential (usually -60 mV); for DSE, the step was 10 s. For DSE, picrotoxin was included in the ACSF. Atropine was obtained from Research Biomedical International (RBI); LY341495, WIN55212-2, and AM404 were from Tocris. SR141716A was obtained from SRI International (Palo Alto, CA) through the National Institute of Mental Health's Chemical Synthesis and Drug Supply Program; ω-agatoxin TK was from Sigma.

#### Analysis

Recordings were filtered at 3 kHz before digitization at 20 kHz using Strathclyde Electrophysiology Software (courtesy of Dr. J. Dempster, University of Strathclyde) and Synapse software (courtesy of Dr. Y. De Koninck, McGill University). Statistical analyses (most often a t test) were performed with SigmaPlot or SPSS, with a level of significance of  $p < 0.05$ . Data are presented as mean ± SEM, and "n" is the number of recorded cells (or, in some experiments, the number of animals).

#### Double-Label Immunocytochemistry

Double-label immunostaining was performed as described previously (Katona et al., 2000). In brief, control and HT littermate pairs were perfused 6 or 7 days post-HT with 4% paraformaldehyde, 0.2% picric acid, and 0.1% glutaraldehyde. Sections were cut at 50 μm, cryoprotected in 30% sucrose/10% glycerol solution, and freeze thawed over liquid nitrogen. Sections were washed, blocked in 2.5% bovine serum albumin solution, and incubated for 48 hr at 4°C in rabbit anti-CB1 (1:1500; raised against the C terminus; Hájos et al., 2000) in combination with either mouse anti-cholecystokinin (CCK) antibody (1:3000; Antibody 9303 kindly provided by CURE/Digestive Diseases Research Center/RIA Core, NIH grant #DK41301) or mouse anti-parvalbumin (PV) antibody (1:2000; Antibody P-3171 Sigma, Saint Louis, MO). The laboratory or company of origin previously confirmed the specificity of each antibody. The sections were washed, incubated for 1 hr in a combination of donkey Cy-3-conjugated anti-rabbit IgG (1:200) and goat FITC-conjugated anti-mouse IgG (1:200; both from Jackson ImmunoResearch, West Grove, PA), washed again, and mounted using Vectashield (Vector Laboratories, Burlingame, CA). Each antibody was also used individually on control sections to verify that there was no bleed-through immunoreactivity.

#### Electron Microscopy and Preembedding Immunogold Techniques

Fifty micrometer sections were incubated with the antibody against the CB1 receptor (see above; 1:1000 for immunogold; 1:6000 for 3,3'-diaminobenzidine [DAB]) for 48 hr, followed by biotinylated goat-anti-rabbit (1:200) and Elite ABC (1:200). For immunogold staining, tyramid intensification was performed (1:40, 10 min), followed by incubation in a streptavidin-labeled 0.8 nm gold colloidal solution overnight. The sections were osmicated, dehydrated, and embed-

ded in Durcupane. All axonal density calculations were corrected for shrinkage. For electron microscopic analysis of the density of CB1+ synapses, the dissector method (see legend to Figures 6D and 6E) was used, because it is not sensitive to potential changes in the size of the examined objects (West, 1999). The number of transected CB1+ axonal profiles per unit area was also measured in the electron microscope, and it was also independently determined from the preembedding immunogold material at the light microscopic level (due to the large size of the colloidal gold particle, the staining was confined to the surface of the sections, providing an essentially 2D staining pattern ideal for quantitative sampling). From the immunogold material, 24 samples (200 μm × 300 μm areas) per each animal were digitally photographed and background subtracted using a high-pass filter (NIHImage). In the resulting binary images, the CB1+ axonal profiles (Figures 6F and 6G) were counted (note that only the number, not the size or staining intensity, of the CB1+ profiles could be determined with this technique).

#### High-Performance Liquid Chromatography/Mass Spectrometry

The HPLC/MS experiments were conducted as described previously (Dinh et al., 2002; Giuffrida et al., 2000). In brief, hippocampi from control and postseizure rats were immediately frozen and homogenized in methanol. Lipids were extracted with chloroform:methanol (2:1, v/v). Samples were centrifuged (3000 rpm) for 5 min, and the organic phase was recovered and evaporated under a stream of N<sub>2</sub> gas. Lipids were resuspended in 1 ml of chloroform and purified over silica columns. Samples were loaded onto silica columns, washed with 1 ml chloroform, and eluted with 2 ml of a mixture of chloroform:methanol (9:1, v/v). Samples were then evaporated under N<sub>2</sub> gas and resuspended in 100 μl of a mixture of chloroform:methanol (2:3, v/v). HPLC/MS analyses were conducted as described (Dinh et al., 2002). <sup>3</sup>H<sub>3</sub>-labeled fatty ethanolamides were synthesized in the laboratory, and 2-[<sup>3</sup>H]<sub>3</sub>JAG was purchased from Cayman Chemical (Ann Arbor, MI).

#### Enzyme Activity Assays

MGL and FAAH assays were performed as described (Dinh et al., 2002; Kathuria et al., 2003). In brief, 50 μg of protein from hippocampal homogenates was incubated in 50 mM tris buffer (pH 7.4) containing 0.5 mg/ml BSA in final volume of 0.5 ml for 30 min at 37°C with arachidonoyl-[<sup>3</sup>H]ethanolamide (10 μM; 10,000 cpm) (for FAAH) or with 2-oleoyl-[<sup>3</sup>H]glycerol (10 μM; 50,000 cpm) (both from American Radiolabeled Chemicals) (for MGL). The reaction was stopped, and products were separated by organic solvent extraction (chloroform:methanol, 1:1); the aqueous phase was taken for radioactive measurements by scintillation counting.

#### Western Blots

Hippocampi were rapidly dissected out and homogenized in 5-fold (volume/weight) excess buffer containing 25 mM HEPES, 10 mM EDTA, 6 mM MgCl<sub>2</sub>, 100 μM PMSF, 10 μM leupeptin, 100 μM benzamide, 10 μM aprotinin (pH 7.4). Homogenates were centrifuged for 5 min at 1000 × g, the supernatants were saved, and the pellets were rehomogenized in buffer and centrifuged as above. The protein concentrations of the combined supernatants were determined using Bio-Rad protein assay. Proteins (40 μg) from each animal were separated by SDS-PAGE and transferred to nitrocellulose. Western blot analysis was performed blind with respect to animal treatment using an antibody raised against the last 14 amino acids of rat CB1 fused to glutathione S-transferase (CB1 L14; 1:250). The antibody was purified and specificity verified as described in Katona et al. (2000). Specific binding was blocked by preincubation of CB1 antiserum with excess fusion protein used for immunization. To ensure equal loading of proteins, the upper portion of the blot containing the higher molecular weight proteins was probed with antibodies (Sigma) to neurofilament polypeptides with apparent molecular weight of 68 kDa, 160 kDa, and 200 kDa, respectively. Radioactivity was quantified using a PhosphorImager (Molecular Dynamics).

#### Acknowledgments

We thank R. Zhu and S. Kathuria for technical assistance; and Drs. N. Lambert and D. Lewis for discussions. This work was supported

by NIH grant NS38580 (to I.S.) and by grants NS33213 (to M.S.), DA12447, and DA3412 (to D.P.) and DA11322 and DA00286 (to K.M.).

Received: February 19, 2003  
Revised: June 23, 2003  
Accepted: July 17, 2003  
Published: August 13, 2003

## References

- Ameri, A., Wilhelm, A., and Simmet, T. (1999). Effects of the endogenous cannabinoid, anandamide, on neuronal activity in rat hippocampal slices. *Br. J. Pharmacol.* **126**, 1831–1839.
- Beau, F.E., and Alger, B.E. (1998). Transient suppression of GABA<sub>A</sub>-receptor-mediated IPSPs after epileptiform burst discharges in CA1 pyramidal cells. *J. Neurophysiol.* **79**, 659–669.
- Beltramo, M., Stella, N., Calignano, A., Lin, S.Y., Makriyannis, A., and Piomelli, D. (1997). Functional role of high-affinity anandamide transport, as revealed by selective inhibition. *Science* **277**, 1094–1097.
- Bouaboula, M., Perrachon, S., Milligan, L., Canat, X., Rinaldi-Carmona, M., Portier, M., Barth, F., Calandra, B., Pecceu, F., Lupker, J., et al. (1997). A selective inverse agonist for central cannabinoid receptor inhibits mitogen-activated protein kinase activation stimulated by insulin or insulin-like growth factor 1. Evidence for a new model of receptor/ligand interactions. *J. Biol. Chem.* **272**, 22330–22339.
- Brooks-Kayal, A.R., Shumate, M.D., Jin, H., Rikhter, T.Y., and Coulter, D.A. (1998). Selective changes in single cell GABA<sub>A</sub> receptor subunit expression and function in temporal lobe epilepsy. *Nat. Med.* **4**, 1166–1172.
- Chen, H., and Lambert, N.A. (2000). Endogenous regulators of G protein signaling proteins regulate presynaptic inhibition at rat hippocampal synapses. *Proc. Natl. Acad. Sci. USA* **97**, 12810–12815.
- Chen, K., Baram, T.Z., and Soltesz, I. (1999). Febrile seizures in the developing brain result in persistent modification of neuronal excitability in limbic circuits. *Nat. Med.* **5**, 888–894.
- Chen, K., Aradi, I., Thon, N., Eghbal-Ahmadi, M., Baram, T.Z., and Soltesz, I. (2001). Persistently modified h-channels after complex febrile seizures convert the seizure-induced enhancement of inhibition to hyperexcitability. *Nat. Med.* **7**, 331–336.
- Chevalyere, V., and Castillo, P.E. (2003). Heterosynaptic LTD of hippocampal GABAergic synapses: a novel role of endocannabinoids in regulating excitability. *Neuron* **38**, 461–472.
- Clement, A.B., Hawkins, E.G., Lichtman, A.H., and Cravatt, B.F. (2003). Increased seizure susceptibility and proconvulsant activity of anandamide in mice lacking fatty acid amide hydrolase. *J. Neurosci.* **23**, 3916–3923.
- Cravatt, B.F., Giang, D.K., Mayfield, S.P., Boger, D.L., Lerner, R.A., and Gilula, N.B. (1996). Molecular characterization of an enzyme that degrades neuromodulatory fatty-acid amides. *Nature* **384**, 83–87.
- Desarnaud, F., Cadas, H., and Piomelli, D. (1995). Anandamide amidohydrolase activity in rat brain microsomes. Identification and partial characterization. *J. Biol. Chem.* **270**, 6030–6035.
- Di Marzo, V., Fontana, A., Cadas, H., Schinelli, S., Cimino, G., Schwartz, J.C., and Piomelli, D. (1994). Formation and inactivation of endogenous cannabinoid anandamide in central neurons. *Nature* **372**, 686–691.
- Dinh, T.P., Carpenter, D., Leslie, F.M., Freund, T.F., Katona, I., Sensi, S.L., Kathuria, S., and Piomelli, D. (2002). Brain monoglyceride lipase participating in endocannabinoid inactivation. *Proc. Natl. Acad. Sci. USA* **99**, 10819–10824.
- Egertová, M., Giang, D.K., Cravatt, B.F., and Elphick, M.R. (1998). A new perspective on cannabinoid signalling: complementary localization of fatty acid amide hydrolase and the CB1 receptor in rat brain. *Proc. R. Soc. Lond. B. Biol. Sci.* **265**, 2081–2085.
- Fitzjohn, S.M., Bortolotto, Z.A., Palmer, M.J., Doherty, A.J., Ornstein, P.L., Schoepp, D.D., Kingston, A.E., Lodge, D., and Collingridge, G.L. (1998). The potent mGlu receptor antagonist LY341495 identifies roles for both cloned and novel mGlu receptors in hippocampal synaptic plasticity. *Neuropharmacology* **37**, 1445–1458.
- Giuffrida, A., Rodriguez de Fonseca, F., and Piomelli, D. (2000). Quantification of bioactive acylethanolamides in rat plasma by electrospray mass spectrometry. *Anal. Biochem.* **280**, 87–93.
- Hájos, N., and Freund, T.F. (2002). Pharmacological separation of cannabinoid sensitive receptors on hippocampal excitatory and inhibitory fibers. *Neuropharmacology* **43**, 503–510.
- Hájos, N., Katona, I., Naiem, S.S., MacKie, K., Ledent, C., Mody, I., and Freund, T.F. (2000). Cannabinoids inhibit hippocampal GABAergic transmission and network oscillations. *Eur. J. Neurosci.* **12**, 3239–3249.
- Hampson, R.E., Zhuang, S.-Y., Weiner, J.L., and Deadwyler, S.A. (2003). Functional significance of cannabinoid-mediated, depolarization-induced suppression of inhibition (DSI) in the hippocampus. *J. Neurophysiol.* **90**, 55–65.
- Hoffman, A.F., and Lupica, C.R. (2000). Mechanisms of cannabinoid inhibition of GABA(A) synaptic transmission in the hippocampus. *J. Neurosci.* **20**, 2470–2479.
- Freund, T.F., and Buzsáki, G. (1996). Interneurons of the hippocampus. *Hippocampus* **6**, 347–470.
- Holmes, G.L., and Ben-Ari, Y. (1998). Seizures in the developing brain: Perhaps not so benign after all. *Neuron* **21**, 1231–1234.
- Kathuria, S., Gaetani, S., Fegley, D., Valino, F., Duranti, A., Tontini, A., Mor, M., Tarzia, G., Rana, G.L., Calignano, A., et al. (2003). Modulation of anxiety through blockade of anandamide hydrolysis. *Nat. Med.* **9**, 76–81.
- Katona, I., Sperlagh, B., Sik, A., Kafalvi, A., Vizi, E.S., Mackie, K., and Freund, T.F. (1999). Presynaptically located CB1 cannabinoid receptors regulate GABA release from axon terminals of specific hippocampal interneurons. *J. Neurosci.* **19**, 4544–4558.
- Katona, I., Sperlagh, B., Magloczky, Z., Santha, E., Kofalvi, A., Czirkak, S., Mackie, K., Vizi, E.S., and Freund, T.F. (2000). GABAergic interneurons are the targets of cannabinoid actions in the human hippocampus. *Neuroscience* **100**, 797–804.
- Kim, J., Isokawa, M., Ledent, C., and Alger, B.E. (2002). Activation of muscarinic acetylcholine receptors enhances the release of endogenous cannabinoids in the hippocampus. *J. Neurosci.* **22**, 10182–10191.
- Kreitzer, A.C., and Regehr, W.G. (2001). Retrograde inhibition of presynaptic calcium influx by endogenous cannabinoids at excitatory synapses onto Purkinje cells. *Neuron* **29**, 717–727.
- McBain, C.J., and Fisahn, A. (2001). Interneurons unbound. *Nat. Rev. Neurosci.* **2**, 11–23.
- Nusser, Z., Hájos, N., Somogyi, P., and Mody, I. (1998). Increased number of synaptic GABA(A) receptors underlies potentiation at hippocampal inhibitory synapses. *Nature* **395**, 172–177.
- Ohno-Shosaku, T., Maejima, T., and Kano, M. (2001). Endogenous cannabinoids mediate retrograde signals from depolarized postsynaptic neurons to presynaptic terminals. *Neuron* **29**, 729–738.
- Ohno-Shosaku, T., Tsubokawa, H., Mizushima, I., Yoneda, N., Zimmer, A., and Kano, M. (2002). Presynaptic cannabinoid sensitivity is a major determinant of depolarization-induced retrograde suppression at hippocampal synapses. *J. Neurosci.* **22**, 3864–3872.
- Pan, X., Ikeda, S.R., and Lewis, D.L. (1998). SR 141716A acts as an inverse agonist to increase neuronal voltage-dependent Ca<sup>2+</sup> currents by reversal of tonic CB1 cannabinoid receptor activity. *Mol. Pharmacol.* **54**, 1064–1072.
- Piomelli, D., Giuffrida, A., Calignano, A., and Rodriguez de Fonseca, F. (2000). The endocannabinoid system as a target for therapeutic drugs. *Trends Pharmacol. Sci.* **21**, 218–224.
- Pitler, T.A., and Alger, B.E. (1992). Postsynaptic spike firing reduces synaptic GABA<sub>A</sub> responses in hippocampal pyramidal cells. *J. Neurosci.* **12**, 4122–4132.
- Rinaldi-Carmona, M., Barth, F., Heaulme, M., Shire, D., Calandra, B., Congy, C., Martinez, S., Maruani, J., Neliat, G., Caput, D., Ferrera, P., Soubrie, P., Breliere, J.C., and Le Fur, G. (1994). SR141716A, a potent and selective antagonist of the brain cannabinoid receptor. *FEBS Lett.* **350**, 240–244.

- Shinnar, S. (1998). Prolonged febrile seizures and mesial temporal sclerosis. *Ann. Neurol.* *43*, 411–412.
- Stella, N., Schweitzer, P., and Piomelli, D. (1997). A second endogenous cannabinoid that modulates long-term potentiation. *Nature* *388*, 773–778.
- Toth, Z., Xiao-Xin, Y., Haftoglou, S., Ribak, C.E., and Baram, T.Z. (1998). Seizure-induced neuronal injury: vulnerability to febrile seizures in an immature rat model. *J. Neurosci.* *18*, 4285–4294.
- Tsou, K., Mackie, K., Sanudo-Pena, M.C., and Walker, J.M. (1999). Cannabinoid CB1 receptors are localized primarily on cholecystikinin-containing GABAergic interneurons in the rat hippocampal formation. *Neuroscience* *93*, 969–975.
- Varma, N., Carlson, G.C., Ledent, C., and Alger, B.E. (2001). Metabotropic glutamate receptors drive the endocannabinoid system in hippocampus. *J. Neurosci.* *21*, RC188.
- Varma, N., Brager, D., Morishita, W., Lenz, R.A., London, B., and Alger, B. (2002). Presynaptic factors in the regulation of DSI expression in hippocampus. *Neuropharmacology* *43*, 550–562.
- Vasquez, C., and Lewis, D.L. (1999). The CB1 cannabinoid receptor can sequester G-proteins, making them unavailable to couple to other receptors. *J. Neurosci.* *19*, 9271–9280.
- Walker, M.C., and Kullmann, D.M. (1999). Febrile convulsions: a 'benign' condition? *Nat. Med.* *5*, 871–872.
- Wallace, M.J., Martin, B.R., and DeLorenzo, R.J. (2002). Evidence for a physiological role of endocannabinoids in the modulation of seizure threshold and severity. *Eur. J. Pharmacol.* *452*, 295–301.
- West, M.J. (1999). Stereological methods for estimating the total number of neurons and synapses: issues of precision and bias. *Trends Neurosci.* *22*, 51–61.
- Wilson, R.I., and Nicoll, R.A. (2001). Endogenous cannabinoids mediate retrograde signalling at hippocampal synapses. *Nature* *410*, 588–592.
- Wilson, R.I., Kunos, G., and Nicoll, R.A. (2001). Presynaptic specificity of endocannabinoid signaling in the hippocampus. *Neuron* *31*, 453–462.